Electromagnetic detection of ultrasonic shear waves in superconducting tin*

R. L. Thomas,† M. J. Lea, E. J. Sendezera,† and E. R. Dobbs
Department of Physics, Bedford College, University of London, London NW1 4NS, England

K. C. Lee‡ and A. M. de Graaf
Department of Physics, Wayne State University, Detroit, Michigan 48202

(Received 25 June 1976)

Measurements of the efficiency of electromagnetic detection and generation of ultrasonic shear waves in superconducting tin are presented. Theoretical calculations of the generation efficiency are given, based upon a model by Quinn. Similar calculations are made for the radiation (detection) efficiency by adapting the Pippard model for ultrasonic shear wave attenuation, and lead to an identical temperature dependence as that predicted for the generation efficiency. Excellent agreement with this predicted behavior is found for experimental observations of the radiation efficiency for an electropolished (001) surface in tin at 15.3 MHz, using a single adjustable parameter. This parameter corresponds to a value of the London penetration depth $\lambda_L(0) = 253 \pm 25$ Å, in agreement with values found in the literature. The experimental generation efficiency is found to be strongly power dependent and is described theoretically by adapting the theory to the case of the intermediate superconducting state established at the surface by the rf magnetic field. Experimental radiation efficiencies are also found to be very sensitive to surface damage, a fact which is attributed to collision drag of the electrons by the lattice in the damaged layer. The theory, modified to allow for surface damage, gives reasonable agreement with experimental radiation efficiencies for etched and spark-planed surfaces.

I. INTRODUCTION

In recent years the electromagnetic generation of ultrasonic shear waves has been investigated experimentally and theoretically for several pure metals and semimetals in the normal state. For a free-electron metal such as potassium,[1] shear waves are generated in the absence of an external magnetic field by the self-consistent electric fields acting upon the lattice ions in the bulk of the metal. In the case of a compensated metal[2] or semimetal,[3] the corresponding shear-wave generation is dominated by the collision-drag forces of both sets of carriers on the lattice atoms. Theoretical calculations[2,3] have been based on a model by Quinn,[4] and are generally in good agreement with experiments for frequencies of the order of 10 MHz.

Studies of the modification of the generation efficiency in the superconducting state have concentrated primarily on pure thin films at microwave frequencies.[5,6] In this experimental regime it is expected that the breakdown of screening of the electromagnetically generated current by the electrons in the bulk[7] will cause the self-consistent electromagnetic field in the interior to become very small, resulting in a very small generation efficiency. It has been suggested[6] that the dominant mechanism for generation in thin films at 9 GHz is diffuse surface scattering.

Some of us have recently reported preliminary results of the first such experiments in a bulk single crystal of tin at 15.3 MHz in the superconducting state.[8] In the course of these experiments it was learned that in order to study the intrinsic behavior of the physical mechanism in a bulk superconductor, it is necessary to measure the efficiency of detection (radiation efficiency) rather than the generation efficiency, because of the perturbing effect of applied rf fields on the superconducting state near T_c. The geometry of the detection mechanism lends itself rather well to a theoretical consideration based upon the Pippard model for ultrasonic attenuation,[7] coupled with theoretical expressions for the self-consistent fields first derived by Fossheim,[9] in considering the attenuation of ultrasonic shear waves in a superconductor. It will be seen in Sec. II that the Pippard model leads to a radiation efficiency which is identical to that calculated on the basis of the Quinn model.[4] In Sec. III we shall describe the experimental technique. In Sec. IV we present experimental radiation efficiencies for electropolished surfaces, and find excellent agreement with the theory described in Sec. II. Generation efficiencies of such surfaces are also described in Sec. IV, and are found to be power dependent. Adapting the theory of Sec. II to the case of the intermediate superconducting state, we are able to account qualitatively for the observed power dependence. Experimental radiation efficiencies were found to depend strongly on surface damage. In Sec. IV we show that the observed behavior may be attributed to the fact that in the damaged surface layer the self-consistent electric fields tend to zero, owing to the collision drag of the electrons by the lattice. We show representative data for etched and spark-planed sur-

faces, and compare these data with the theory of Sec. II, modified to incorporate the screening of the internal electric fields by the damaged superconducting layer, and find satisfactory agreement.

II. THEORETICAL CONSIDERATIONS

A. Generation efficiency—Quinn approach

The purpose of this section is to construct a theoretical model of the electromagnetic generation of sound in a bulk type-I superconductor. No first-principles calculations of the electromagnetic generation of sound in bulk type-I superconductors have been reported in the literature, except for a brief calculation in a recent note by some of the present authors.[10] Although Abelès,[5] and later Goldstein and Zemel,[6] have addressed themselves rather extensively to this problem, their treatment was specifically tailored to fit the case of superconducting thin films, *not* bulk superconductors. In the view of those authors, the electromagnetic generation of sound, in thin films at least, is entirely due to surface scattering. In the present paper we shall treat quite a different situation. We have in mind an isotropic free-electron metal which becomes superconducting at a temperature $T = T_c$, occupying the half-space $z > 0$, with an electromagnetic wave impinging on the surface from the vacuum $z < 0$. We shall take the point of view that the electromagnetic generation of sound is solely a result of the force exerted by the self-consistent electric field inside the superconductor on the background of positively charged ions. Thus we neglect possible contributions to the generation efficiency from surface scattering or collision-drag mechanisms by assuming that the surface scattering is specular, and the electron mean free path is sufficiently large. These are admittedly rather stringent conditions, but the theoretical framework becomes very simple, and as we shall show, excellent agreement with our experimental results is obtained.

Assuming that all field quantities vary as $\exp(i\omega t - iqz)$, Maxwell's equations lead to

$$E_x(q,\omega) = \frac{-i\mu_0\omega}{q^2} j_x(q,\omega) + \frac{i\omega}{\pi q^2} B_y(0^+),$$

$$E_y(q,\omega) = \frac{-i\mu_0\omega}{q^2} j_y(q,\omega) - \frac{i\omega}{\pi q^2} B_x(0^+), \tag{1}$$

where $B_x(0^+)$ and $B_y(0^+)$ are the components of the magnetic induction of the electromagnetic wave at the surface of the superconductor, and j_x and j_y are the components of the total current density. Defining a transverse electric field $E_t = E_x\hat{i} + E_y\hat{j}$, where $\hat{i}$ and $\hat{j}$ are unit vectors along the x and y axes parallel to the surface of the superconductor, we can rewrite Eq. (1) as

$$E_t(q,\omega) = \frac{-i\mu_0\omega}{q^2} j_t(q,\omega) + \frac{i\omega}{\pi q^2}\tilde{T}B_t(0^+), \tag{2}$$

where $\tilde{T}$ is the rotation operator given by

$$\tilde{T} = \begin{pmatrix} 0 & 1 \\ -1 & 0 \end{pmatrix}.$$

The equation of motion of the (isotropic) background of the superconductor is

$$\rho\ddot{\xi}_t = G\frac{d^2\xi_t}{dz^2} + n_i Ze E_t, \tag{3}$$

where ξ_t is the transverse elastic displacement field, ρ is the density of the superconductor, and G is the shear modulus. The last term on the right represents the coupling of the positive elastic background with the self-consistent electric field inside the superconductor. Z is the valence of the ions and n_i is the number of ions per unit volume. For a metal, $n_i Z \equiv n$, where n is the conduction-electron concentration. Since in this paper we are only interested in transverse acoustic waves, Eq. (3) contains no longitudinal elastic terms. Since all field quantities vary as $\exp(i\omega t - iqz)$, we may rewrite Eq. (3) as

$$\xi_t(q,\omega) = \frac{ne}{\rho(s^2q^2 - \omega^2)} E_t(q,\omega), \tag{4}$$

where $s = (G/\rho)^{1/2}$ is the velocity of transverse sound in the superconductor.

Finally we set

$$j_t(q,\omega) = \sigma_S(q,\omega)E_t(q,\omega) + nei\omega\xi_t(q,\omega), \tag{5}$$

where $\sigma_S(q,\omega)$ is the wave-number- and frequency-dependent transverse electronic conductivity of the superconductor, and the last term represents the contribution of the ionic current density. Combining Eqs. (2), (4), and (5), and transforming $\xi_t(q,\omega)$ to real space, we obtain

$$\xi_t(z,t) = \frac{nei\omega}{\pi\rho}\tilde{T}B_t(0^+) \times\int_{-\infty}^{+\infty} \frac{\delta_S^2 e^{i(\omega t - qz)}\,dq}{(q^2s^2 - \omega^2)(q^2\delta_S^2 + i) - \omega n^2e^2/\rho\sigma_S}, \tag{6}$$

where we have defined $\delta_S^{-2} = \mu_0\omega\sigma_S$. At frequencies of the order of 10 MHz, the last term in the denominator of the integrand may be neglected. The integrand in Eq. (6) possesses two acoustic poles, and poles corresponding to highly damped modes. We are only interested in the acoustic mode traveling in the positive z direction. Its

form is given by

$$\xi_t(z,t) = -\frac{ne}{\rho s}\,\bar{T}B_t(0^+)\,\frac{e^{i\omega(t-z/s)}}{q_A^2 + i\mu_0\omega\sigma_S}\,, \tag{7}$$

where σ_S is evaluated at $q = q_A \equiv \omega/s$. We define

$$\sigma_S = \sigma_{1S} - i\sigma_{2S} \tag{8}$$

and

$$\delta_N = (\mu_0\omega\sigma_N)^{-1/2}, \tag{9}$$

where σ_N is the conductivity in the normal state, and where δ_N is an effective skin depth characterizing the degree of screening of the electromagnetically generated current by the electrons.[7] The generation efficiency of the superconductor Γ_S is defined to be the ratio of the acoustic flux leaving the surface to the electromagnetic flux incident on the surface, i.e.,

$$\Gamma_S = \frac{\frac{1}{2}\rho s\omega^2|\,\xi_t(0^+)|^2}{\frac{1}{8}c/\mu_0|\,B_t(0^+)|^2}\,, \tag{10}$$

where we have made use of the boundary condition $B_t(0^+) = 2B_t$ (incident). Using Eqs. (7)–(10), we find

$$\Gamma_S = \frac{4\mu_0\omega^2 n^2 e^2}{\rho sc}\,\frac{\delta_N^4}{(q_A^2\delta_N^2 + \sigma_{2S}/\sigma_N)^2 + (\sigma_{1S}/\sigma_N)^2}\,. \tag{11}$$

In the normal state, Eq. (11) becomes

$$\Gamma_N = \frac{4\mu_0\omega^2 n^2 e^2}{\rho sc}\,\frac{\delta_N^4}{q_A^4\delta_N^4 + 1}\,, \tag{12}$$

so that the ratio of Γ_S to Γ_N is given by

$$\frac{\Gamma_S}{\Gamma_N}\,\frac{q_A^4\delta_N^4 + 1}{(q_A^2\delta_N^2 + \sigma_{2S}/\sigma_N)^2 + (\sigma_{1S}/\sigma_N)^2}\,. \tag{13}$$

In Eqs. (11)–(13), the conductivities are evaluated at $q = q_A \equiv \omega/s$. Equation (13) was first derived in Ref. 8 from the expressions for the self-consistent electromagnetic fields developed by Fossheim[9] in discussing the ultrasonic attenuation in a superconductor. It should be noted that Eq. (12) is identical to that obtained by Mertsching,[11] who generalized a previous calculation by Alig[12] for the normal state.

B. Radiation efficiency—Pippard approach

The inverse of the generation of sound described above is the radiation of electromagnetic energy which occurs when transverse sound propagating in a metal is reflected from the surface. The purpose of this section is to give a derivation of the radiation efficiency and show that it is identical to the generation efficiency given in Sec. II A.

We shall consider an undamped transverse sound wave $\xi_t(z,t) \sim \exp(i\omega t - iq_A z)$ incident from the left on a metal surface at $z = 0$. From Maxwell's equations and Eq. (5) we have

$$q^2 E_t(q,\omega) = -i\mu_0\omega[\sigma_S(q,\omega)E_t(q,\omega) + ne\,i\omega\xi_t(q,\omega)]\,. \tag{14}$$

Solving for $E_t(q,\omega)$, transforming to real space, and using Eq. (8), we obtain

$$E_t(z,t) = \frac{\mu_0 ne\omega^2\xi_t(z,t)}{q_A^2 + i\mu_0\omega(\sigma_{1S} - i\sigma_{2S})}\,. \tag{15}$$

The radiation efficiency of the superconductor, H_S, is defined as the ratio of the electromagnetic flux leaving the surface to the acoustic flux incident on the surface, i.e.,

$$H_S = \frac{\frac{1}{2}c\epsilon_0|\,E_t(0^+)|^2}{\frac{1}{2}\rho s\omega^2|\,\xi_t(0^-)|^2}\,. \tag{16}$$

Here we have made use of the acoustic boundary condition which gives rise to an antinode at a free surface. Using Eqs. (9), (15), and (16), together with the boundary condition which requires that $E_t(0^+) = E_t(0^-)$, we obtain

$$H_S = \frac{\mu_0\omega^2 n^2 e^2}{4\rho sc}\,\frac{\delta_N^4}{(q_A^2\delta_N^2 + \sigma_{2S}/\sigma_N)^2 + (\sigma_{1S}/\sigma_N)^2}\,, \tag{17}$$

which is equal to Γ_S, as given by Eq. (11). In the normal state the radiation efficiency H_N is, therefore, equal to Γ_N, as given by Eq. (12).

III. EXPERIMENTAL TECHNIQUE

Experimental measurements were made of Γ_S/Γ_N and of H_S/H_N as a function of temperature on a single crystal of tin for frequencies in the range 15–45 MHz. The crystal was machined in the form of a right circular cylinder by spark erosion. The cylinder was 9.5 mm in diameter and 12 mm long, with its faces parallel to (001) crystallographic planes. The faces were prepared with various depths of surface damage between experimental runs by using different energies of spark discharge. Measurements were also made on electropolished surfaces, which best approximated the condition of surface specularity assumed in developing the theory presented in Sec. II. These surfaces were prepared initially by spark planing at the lowest available energy. Next, a perchloric-acid–anhydride mixture was used for electropolishing, following a procedure described by Tai *et al.*[13] Only the results of measurements taken on electropolished surfaces are compared directly with the theoretical prediction of Eq. (13).

Since the generation efficiency in the normal state expected from Eq. (12) is very small (~ -100

dB), the design of the rf coil was found to be an important factor in achieving a signal sufficiently strong to carry out the experiment in the superconducting state. Previous experiments[1,2] have utilized rf coils in the form of a finite-length solenoid to generate linearly polarized shear waves. Such coils have rather poor efficiencies, however, since the rf fields outside the coil are exponentially decaying. The rf-coil geometry which was used in our experiments is shown schematically in Fig. 1. The section of the coil which is pressed lightly against the surface of the specimen consists of eight parallel wires. The wires in this section are packed closely together in a slot in the cylindrical copper mount and are backed by a layer of dielectric material. The return loops of the coil are bent away in a groove in the side of the mount, so that the center of the sample surface is kept as far away as possible, and shielded from the returning currents in the coil. This geometry was found to yield considerably better generation efficiency than that of a conventional solenoid, and also provided a well-defined polarization direction. A 5-MHz ac-cut quartz transducer with its polarization direction aligned with the eight parallel wires of the coil was bonded to the opposite surface of the sample. The coil and sample were mounted in a copper cell, together with a carbon resistor thermometer and a small heater, all of which were maintained in direct contact with the liquid-helium bath. The ambient magnetic fields at the position of the sample were cancelled to within approximately 50 mG prior to cooling the specimen to liquid-helium temperatures.

Conventional ultrasonic-pulse-transmission techniques were used, transmitting on the coil and receiving with the quartz transducer to measure Γ_S/Γ_N, and reversing the procedure to measure H_S/H_N. In both cases the superheterodyne receiver was preceded by a tuned low-noise preamplifier. A boxcar integrator was used to monitor the height of the detected signal pulse from the receiver at the time of flight of the sound wave. The dc output of the boxcar integrator was displayed on the y axis of an X-Y recorder. An attenuated comparison pulse of the same frequency and delay time as the signal was developed by a signal generator and fed simultaneously to the input of the preamplifier. With the sample in the normal state, the comparison pulse was attenuated well below the noise level of the receiver. Following a temperature sweep below the superconducting transition, the generation efficiency drops rapidly and the signal pulse drops below noise level. The signal generator was then used to calibrate the signal. In a second temperature sweep the quartz transducer was used alone in pulse reflection, in order to obtain the temperature dependence of the ultrasonic attenuation over the same range of temperatures. The generation signal was then corrected for the attenuation corresponding to its time of flight prior to comparing with Eq. (13).

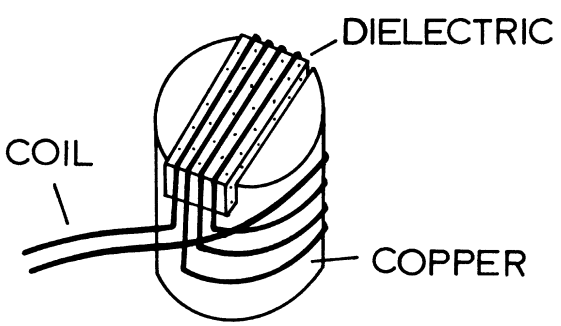

FIG. 1. Schematic diagram of rf-coil geometry.

The carbon resistor thermometer was monitored by means of a resistance bridge, the output of which was displayed on the x axis of the recorder. The thermometer was calibrated by measuring the vapor pressure of the liquid-helium bath as the temperature was lowered.

IV. EXPERIMENTAL RESULTS

A. Radiation efficiency of electropolished surfaces

A typical X-Y recorder trace of the signal detected by the rf coil at 15.3 MHz for an electropolished surface at temperatures close to T_c is shown in Fig. 2. It can be seen that the radiation efficiency drops very rapidly below T_c, having decreased by about 15 dB at $T = 0.99T_c$. For purposes of comparison, it may be noted that the corresponding decrease in attenuation of the propagating sound wave is only about 1 dB. Thus, at 15 MHz, the temperature dependence of the received signal for this sample is dominated by the decrease in radiation efficiency.

In order to make a comparison of the data with the behavior predicted by Eq. (13), it is necessary to estimate the quantities $q_A\delta_N$, σ_{1S}/σ_N, and σ_{2S}/σ_N under the present experimental conditions. Page and Leibowitz[14] have carried out measurements of the electromagnetic part of the shear-wave attenuation at frequencies above 1 GHz, from which they estimate that $\delta_N = 0.23$ μm. This is the limiting value of δ_N for $q_A l \gg 1$, where l is the electron mean free path. Assuming this value for δ_N, and using $s = 1.82\times10^3$ m/sec, we find that $q_A\delta_N \sim 0.01$, so that Eq. (13) may be written

$$\frac{H_S}{H_N} = \frac{1}{(\sigma_{2S}/\sigma_N)^2 + (\sigma_{1S}/\sigma_N)^2} \,. \tag{18}$$

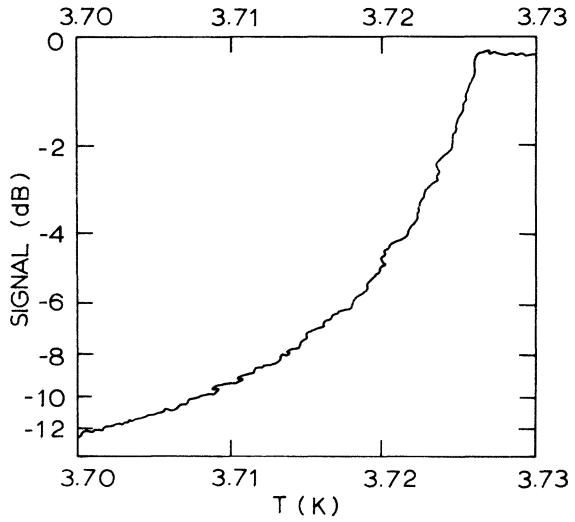

FIG. 2. Recorder tracing of the peak pulse height detected by the rf coil for a 15.3-MHz ultrasonic shear-wave indicent on an electropolished (001) surface for temperatures close to the superconducting transition.

Equation (18) is readily evaluated, provided that $\Delta T \equiv (T_c - T) \ll T_c$, as is the case for our measurements. In this limit we use the approximate expressions for σ_{1S}/σ_N and σ_{2S}/σ_N, as given by Cullen and Ferrell[15]

$$\sigma_{1S}/\sigma_N \simeq 2f(\epsilon) + \tfrac{1}{2}\beta\epsilon \ln(8\epsilon/e\hbar\omega) - 0.853(\beta\epsilon)^2 , \tag{19}$$

and

$$\sigma_{2S}/\sigma_N \simeq 2\delta_N^2 \Delta T/\lambda_L^2(0) T_c ,$$

where $f(\epsilon)$ is the Fermi-Dirac function, $\beta = 1/kT$, ϵ is the temperature dependent superconducting energy gap, e is the base of the natural logarithm, and $\lambda_L(0)$ is the London penetration depth at absolute zero. Equations (18) and (19) show that H_S/H_N can be compared with the experimental data with only one adjustable parameter $\delta_N/\lambda_L(0)$, all other quantities being known for tin.[16] We have plotted $(\sigma_{1S}/\sigma_N)^2$ and $(\sigma_{2S}/\sigma_N)^2$ in Fig. 3 for $\delta_N/\lambda(0) = 15.74$. One sees that for large ΔT, $(\sigma_{2S}/\sigma_N)^2 \gg (\sigma_{1S}/\sigma_N)^2$, so that $H_S/H_N \propto (\Delta T)^{-2}$. At log-log plot of the experimental data is shown in Fig. 4, illustrating this behavior for the radiation efficiency of an electropolished surface. A detailed comparison with Eq. (18) is shown for the electropolished surface in Fig. 5, with $\delta_N/\lambda_L(0) = 15.74 \pm 0.25$. The fit is good over the entire temperature range. Under our experimental conditions, $q_A l = 0.9 \pm 0.2$, as deduced from the observed frequency dependence of the normal-state attenuation. Using this value of $q_A l$, together with Pippard's[7] expression for $\sigma_N(q_A l)$,

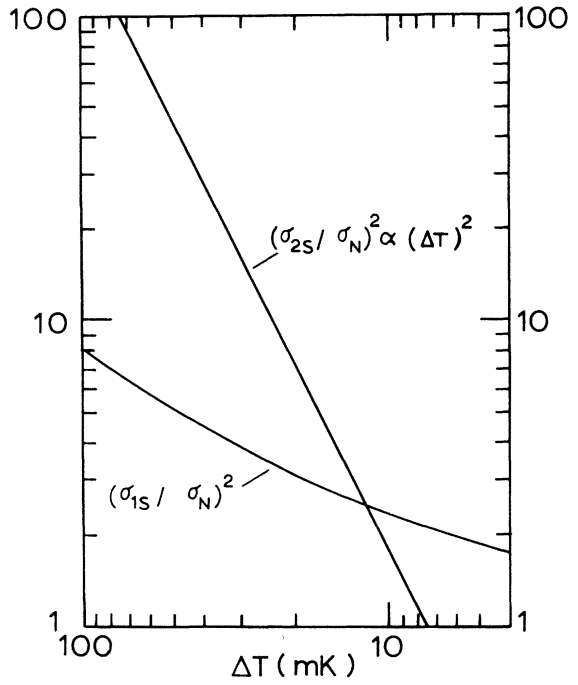

FIG. 3. Log-log plots of $(\sigma_{1S}/\sigma_N)^2$ and $(\sigma_{2S}/\sigma_N)^2$ as a function of $\Delta T = T_c - T$. Note that for large ΔT, $(\sigma_{2S}/\sigma_N)^2$ dominates the behavior of Eq. (18).

we find $\delta_N/\lambda_L(0) = 9.1 \pm 1$ for $q_A l \gg 1$. This value is in good agreement with that of Page and Leibowitz,[14] who find a value of 9.47 for this parameter. If our result is combined with their estimate $\delta_N = 0.23$ μm, we obtain from our data $\lambda_L(0) = (253 \pm 25)$ Å, in good agreement with Page's[14] value of

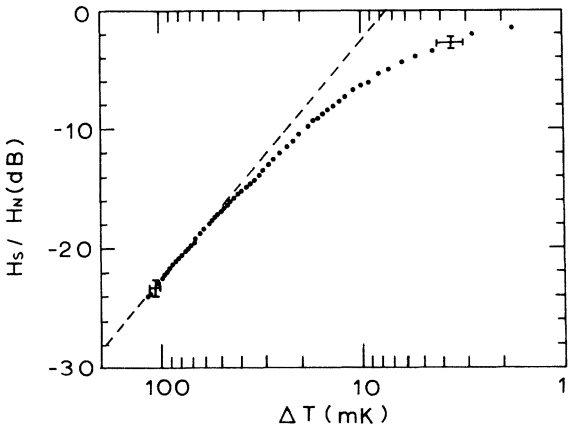

FIG. 4. Log-log plot of the measured radiation efficiency as a function of temperature below T_c at 15.3 MHz for shear waves propagating along [001] in tin. The dashed line shows the expected behavior in the limit of large ΔT. The error bars include an estimate of possible systematic errors.

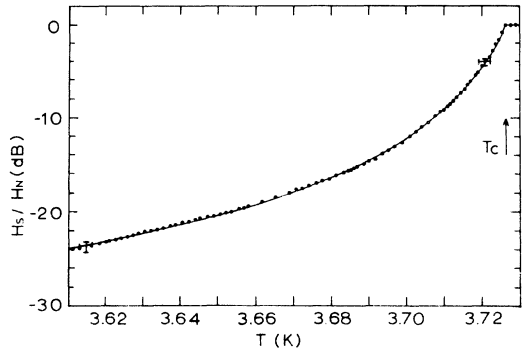

FIG. 5. Comparison of the observed radiation efficiency at 15.3 MHz (points) with Eq. (18) (solid curve). One adjustable parameter, $\delta_N/\lambda_L(0) = 15.74 \pm 0.24$, was used, as described in the text.

243 Å, as well as with Tai *et al.*'s[13] value of 252 Å, which they measured by means of a SQUID technique.

From Eqs. (18) and (19) it can be seen that the frequency dependence of the normalized radiation efficiency is predicted to be weak, provided that $q_A l \gtrsim 1$ and $q_A \delta_N \ll 1$. The data for frequencies of 25, 35 and 45 MHz qualitatively support this conclusion, with temperature dependences similar to that shown in Fig. 5 for 15.3 MHz. Signal-to-noise ratios deteriorated at the higher frequencies, however, and the correction for attenuation became an increasingly larger fraction of the total signal, so that it was not possible to determine quantitatively conclusive trends as a function of frequency for this sample.

B. Generation efficiency–power dependence

Although the theory of Sec. II predicts the temperature dependence of the generation efficiency to be the same as that of the radiation efficiency, experimentally it is found to be very different. Moreover, the temperature dependence of the generation efficiency depends on the power delivered to the coil, as can be seen from Fig. 6. At full power, the signal is observable at all temperatures. As the power to the coil is reduced, the temperature dependence tends towards that observed for the radiation efficiency, although there was not sufficient signal to achieve the asymptotic behavior of the generation, Γ_S/Γ_N. At the lower powers a broad maximum in the temperature dependence may also be noted, which does not appear to be related to the decreasing attenuation of the specimen, as the temperature is lowered. A power dependence of the generation efficiency has also been reported by Goldstein and Zemel[6] in their microwave experiments on the superconducting

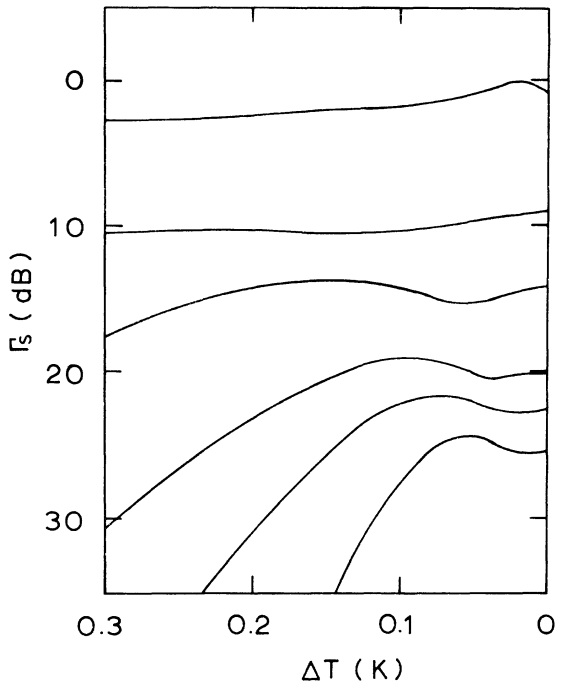

FIG. 6. Temperature dependence of the ultrasonic shear-wave generation efficiency at 15.3 MHz for different rf power levels. The values of $\Gamma_S(0)$ indicate the relative rf power supplied to the coil.

film, and was attributed by them to the rf magnetic field exceeding the critical field $B_c(T)$.

We shall sketch a simple model which accounts qualitatively for the salient features of the power dependence observed in our experiments. Since $B_c(T)$ decreases with increasing temperature, the sample will be in an intermediate state for sufficiently large $B_t(z)$, or sufficiently small ΔT. The field $B_t(z)$ is, of course, very nonuniform, decaying to zero in a length L, so that the interior of the sample remains superconducting. We then assume that this intermediate state may be described as a superconductor with a thin normal surface layer of thickness $L_N < L$. We further assume the conductivity in this intermediate state may be written as $\gamma\sigma_S + (1-\gamma)\sigma_N$, where $\gamma = (L - L_N)/L$. Using the theory of Sec. II A, the generation efficiency becomes

$$\frac{\Gamma_S}{\Gamma_N} = \frac{1}{\gamma^2(\sigma_{2S}/\sigma_N)^2 + [(1-\gamma) + \gamma(\sigma_{1S}/\sigma_N)]^2} \,. \quad (20)$$

In writing Eq. (20) we are neglecting higher-order terms in B_t, emphasizing only its role in creating the intermediate state. In the normal layer the field is given by

$$B_t(z) = B_t(0^+) \exp(-z/\delta_0) \,, \quad (21)$$

where δ_0 is the skin depth in the normal state. At a given temperature, the position $z = L_N$ of the N-S interface is determined by setting $B_t(L_N) = B_c(T) = B_c(0)[1-(T/T_c)^2]$. The fields extend a further distance $L - L_N = \lambda_L(T) = \lambda_L(0)[1-(T/T_c)^2]^{-1/2}$ into the superconducting interior. The expression for γ then becomes

$$\gamma = 1 - \frac{\ln[B_t(0^+)/B_c(T)]}{\lambda_L(T)/\delta_0 + \ln[B_t(0^+)/B_c(T)]}. \tag{22}$$

Equation (22) is restricted to the temperature range for which $B_t(0^+) \geq B_c(T)$, and for which $\lambda_L(T) \leq \delta_0$, so that a normal layer exists, and to take into account the fact that the ac fields decay at least as rapidly in the superconducting region as they do in the normal state. This temperature range is given by

$$[1 - B_t(0^+)/B_c(0)]^{1/2} \leq T/T_c \leq \{1 - [\lambda_L(0)/\delta_0]^2\}^{1/2}. \tag{23}$$

We set $\gamma = 1$ for lower temperatures, and $\gamma = 0$ for higher temperatures. At a frequency of 15 MHz, we estimate $\lambda_L(0)/\delta_0 \approx 0.01$ for our sample. Using Eqs. (19), (20), and (22), we obtain the curves plotted in Fig. 7. It should be noted that the model sketched above predicts a temperature dependence of the generation efficiency with a negative curvature, and a slope which decreases with increasing power in the temperature interval defined in Eq. (23). This behavior compares favorably with the experimental observations (Fig. 6). In contrast, the temperature dependence of the radiation efficiency shows positive curvature throughout the temperature range of interest, and is independent of the transmitter power over the same range of powers.

C. Effects of surface roughness on the radiation efficiency

In Sec. IV A, it was noted in reference to Fig. 4 that for an electropolished surface, H_S/H_N is asymptotically proportional to ΔT^{-2}. If the surface is roughened in any way, however, a faster decrease in H_S/H_N is observed. For example, lightly etching an electropolished surface caused a faster decrease just below T_c and a limiting behavior $H_S/H_N \propto \Delta T^{-2.3}$, as shown in Fig. 8. A finely spark-planed surface yielded an even sharper decrease, with $H_S/H_N \propto \Delta T^{-3.2}$, also shown in Fig. 8. This behavior can be understood if one assumes that in a damaged superconducting layer of depth d, $q_A l < 1$, so that collision-drag effects must be taken into account. The electronic collision-drag current and the ionic current are in opposite directions, and cancel exactly in the limit $q_A l \ll 1$. In this limit (corresponding to a completely damaged region) the self-consistent electric field also tends to zero, resulting in a negligible radiation efficiency for this region. The self-consistent electric field, which is uniform in the interior of

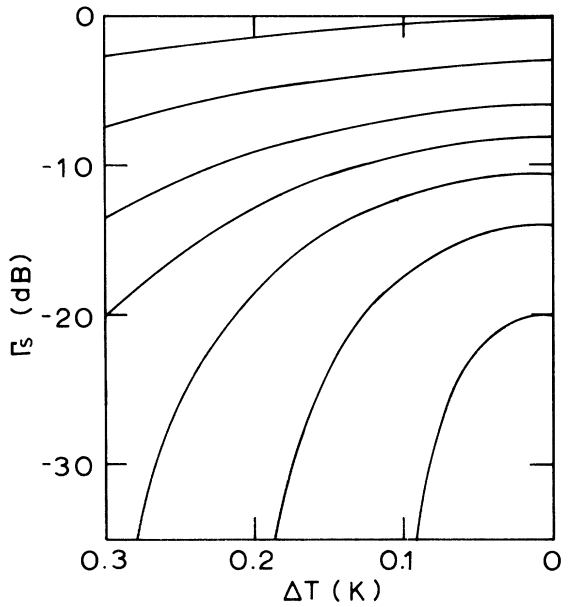

FIG. 7. Theoretical curves for the temperature dependence of the generation efficiency of ultrasonic shear-waves at 15.3 MHz, calculated from Eq. (20). As in Fig. 6, the values of $\Gamma_S(0)$ indicate the relative rf power. For the top curve we take $[B(0^+)/B_c(0)]^2 = 0.25$, and the lower curves are normalized to this value.

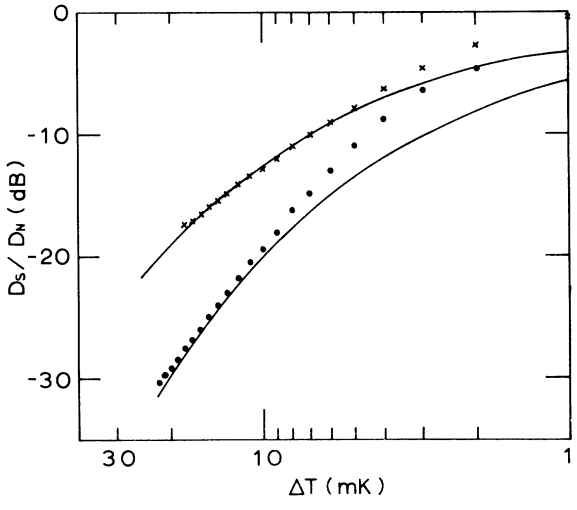

FIG. 8. Log-log plots of the measured radiation efficiency as a function of temperature below T_c at 15.3 MHz for a lightly etched surface (+) and for a spark-planed surface (●). The solid curves are calculated from Eq. (24) using values of assumed surface damage depth, $d = 0.24$ μm (top curve) and $d = 0.54$ μm (bottom curve).

the sample and is given by Eq. (15), will then decay in the damaged layer with the characteristic length $\lambda_L(T)$. The radiation efficiency is, therefore,

$$\frac{D_S}{D_N} = \frac{H_S}{H_N} e^{-2d/\lambda_L(T)} , \tag{24}$$

where D_S/D_N represents the radiation efficiency for the case of a damaged surface, and where H_S/H_N is given by Eq. (18). Equation (24) has been used to fit experimental data for a spark-planed surface, as well as for an etched surface. The results are shown in Fig. 8. The value of $d = 0.54$ μm needed to fit the data for the spark-planed surface is consistent with the damage depth expected for the spark energy used in preparing this surface. The value of $d = 0.24$ obtained for the etched surface is smaller than that for the spark planed surface as one would expect. Radiation efficiency data for more deeply spark planed surfaces show an even more rapid decrease with ΔT, in qualitative agreement with Eq. (24).

---

*Supported in part by the Science Research Council (U.K.) by the U. S. Air Force Office of Scientific Research under Grant No. AFOSR-74-2648, and by the NSF under Grant No. GH 17683.

†Present address: Department of Physics, Wayne State University, Detroit, Mich. 48202.

‡Present address: College of Science, National Central University, Chung-Li, Taiwan, Republic of China.

[1]R. L. Thomas, G. Turner, and D. Hsu, Phys. Lett. A 30, 316 (1969); G. Turner, R. L. Thomas, and D. Hsu, Phys. Rev. B 3, 3097 (1971).

[2]N. K. Batra, R. L. Thomas, K. C. Lee, and A. M. de Graaf, Phys. Rev. B 8, 5473 (1973).

[3]K. C. Lee, A. M. de Graaf, D. Hsu, and R. L. Thomas, Phys. Rev. B 8, 460 (1973).

[4]J. J. Quinn, Phys. Lett. A 25, 522 (1967).

[5]B. Abelès, Phys. Rev. Lett. 19, 1181 (1967).

[6]Y. Goldstein and A. Zemel, Phys. Rev. Lett. 28, 147 (1972); A. Zemel, in *Proceedings of the 1974 Ultrasonics Symposium* (IEEE, New York, 1974).

[7]A. B. Pippard, Proc. R. Soc. A 257, 165 (1960); A. B. Pippard, *The Dynamics of Conduction Electrons* (Gordon and Breach, New York, 1965).

[8]R. L. Thomas, M. J. Lea, E. Sendezera, and E. R. Dobbs, J. Phys. F 5, L21 (1975).

[9]K. Fossheim, Phys. Rev. Lett. 19, 81 (1967).

[10]K. C. Lee, Ph.D. thesis (Wayne State University, 1974) (unpublished); A. M. de Graaf and K. C. Lee, Bull. Am. Phys. Soc. 19, 277 (1974).

[11]J. Mertsching, Phys. Status Solidi 37, 365 (1970).

[12]R. C. Alig, Phys. Rev. 178, 1050 (1969).

[13]P. C. L. Tai, Ph.D. thesis (Harvard University, 1973) (unpublished); P. C. L. Tai, M. R. Beasley, and M. Tinkham, Phys. Rev. B 11, 411 (1975).

[14]E. A. Page, Ph.D. thesis (University of Maryland, 1969) (unpublished); E. A. Page and J. R. Leibowitz (unpublished).

[15]J. R. Cullen and R. A. Ferrell, Phys. Rev. 146, 282 (1966).

[16]We take $T_c = 3.725$ K, and $\epsilon(0) = 1.55 k T_c$ for an (001) surface.